From global to local bifurcations in a forced Taylor-Couette flow.

V. Iranzo*, **F. Marqués, J. M. Lopez**
Department of Applied Physics
Universitat Politècnica de Catalunya, Campus Nord UPC, 08034 Barcelona, Spain
e-mail: iranzo@fa.upc.es

ABSTRACT

Gluing bifurcation is a global bifurcation where two symmetrically related time periodic states simultaneously become homoclinic to an (unstable) saddle state and result in a single symmetric time-periodic state, as a parameter is varied. In a previous paper, [1], the systematic study of gluing bifurcations that had been receiving much attention by this time, [2][3][4], was extended to the unfolding, due to imperfect symmetry, of this kind of bifurcation in a system with Z_2 symmetry generated by a space-time gliding symmetry, i.e. a half period time translation plus a space reflection.

A gluing bifurcation had been found, [2][3], in computed solutions of a temporally forced Taylor-Couette system with aspect ratio 10. The temporal forcing aids in the analysis of the problem in that the Z_2 spatial reflection symmetry of the unforced system is replaced by a spatio-temporal glide reflection symmetry which can be broken in a very controlled and simple manner, i.e. by adding a small multiple of the first temporal harmonic of the forcing, this multiple being the small imperfection parameter.

The gluing bifurcation can be trivially isolated from any $\mathrm{SO}(2)$ symmetry breaking related dynamics by computing in the axisymmetric subspace. This restriction agrees with recent experimental results, [4][5], which indicate that that the dynamics associated with the gluing bifurcation takes place in an $\mathrm{SO}(2)$ invariant subspace, even though the observations of this dynamics come from full 3D solutions.

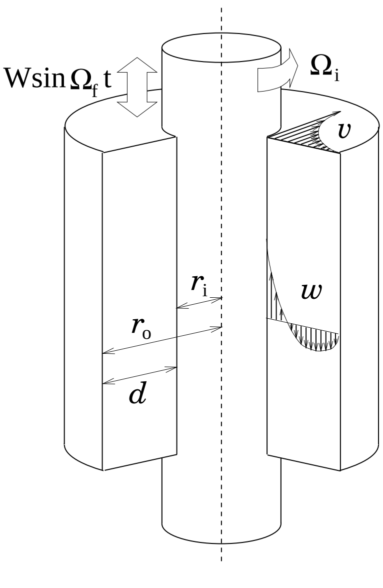

Figure 1: Schematic of the flow configuration

The model problem we consider is the flow between two coaxial finite cylinders with stationary top and bottom end-walls (see Fig 1). The outer cylinder is stationary too while the inner cylinder rotates at constant angular velocity Ω_i and oscillates in the axial direction with velocity $W\sin(\Omega_f t)$. Its radius is r_i, the radius of the outer cylinder is r_o, their length is L and the annular gap between the cylinders is $r_o - r_i$. The nondimensional governing parameters are: the radius ratio $e = r_i/r_o$, the length to gap ratio $\Lambda = L/d$, the Couette flow Reynolds number $Ri = dr_i\Omega_i/\nu$, the axial Reynolds number $Ra = Wd/\nu$, and the nondimensional forcing frequency $\omega_f = d^2\Omega_f/\nu$. The basic flow is time-periodic with period $T_f = 2\pi/\omega_f$, synchronous with the forcing and independent of the azimuthal coordinate.The incompressible Navier-Stokes equations governing this problem are invariant two rotations about the common axis, $SO(2)$, and a temporal glide-reflection Z_2. This Z_2 group is generated by the discrete symmetry S that is a reflection orthogonal to the axis with a simultaneous time translation of a half forcing period and satisfies $S^2 = I$. The groups $SO(2)$ and Z_2 commute for this problem. The equations are solved in an axisymmetric subspace invariant to $SO(2)$, for this reason the only relevant group of symmetry is Z_2.

Because it is very difficult to obtain a pure harmonic oscillation in an experiment, and in presence of any deviation of harmonicity, S ceases to be a symmetry group of the system, an imperfection of the

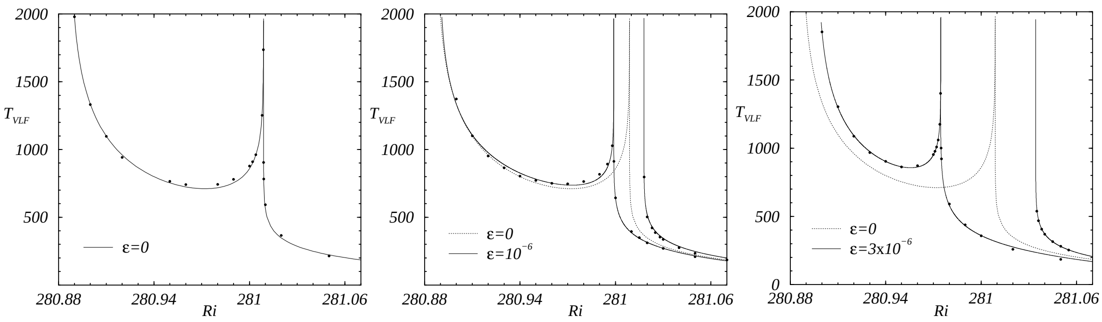

Figure 2: Variation of $\mathrm{T_{VLF}}$ with Ri and ϵ .

harmonic character is considered here. The nonharmonic axial oscillations, here introduced, are given by the expression $W(\sin(\Omega_f t) + \epsilon \sin(2\Omega_f t)$, where ϵ is a measure of the imperfection.

The temporal glide-reflection produces a convoluted scenario in this flow, comprising a gluing of three-tori ($\mathbb{T}^3$) and homoclinic and heteroclinic dynamics, [2][3]. This gluing bifurcation is the organizing center of the dynamics and the cause of spontaneous symmetry breaking in this problem.

The explorations of the parameter space was carried out solving the Navier-Stokes for different values of ϵ and Ri and keeping all other parameters fixed ($\Gamma = 30,\ e = 0.905,\ Ra = 80,\ \omega_f = 30$). For the case $\epsilon = 0$ exists a range of Ri, $Ri \in [280.89, 281.26]$ where stable $\mathbb{T}^3$ solutions exist [2][3]. These $\mathbb{T}^3$ solutions have three incommensurate frequencies: the forcing frequency, $\omega_f = 30$, a second frequency at $\omega_s \simeq 5.2$, and a very low frequency ω_{VLF} which is three orders of magnitude smaller than ω_f.

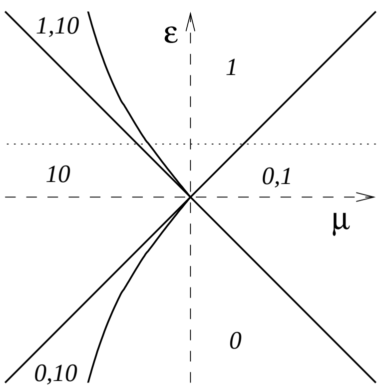

Figure 3: Bifurcation diagram for the unfolding of the gluing bifurcation

For $\epsilon \neq 0$, the $\mathrm{T_{VLF}} \to \infty$ gluing bifurcation splits into three distinct homoclinic bifurcations, as shown in Fig. 2. A classification of the possible gluing bifurcation scenarios and its application to systems with imperfections was obtained and analyzed in Refs. [6],[7] and [8]. The unfolding of the bifurcation is described by two parameters, μ (related to the Reynolds number in this paper) and ϵ, the imperfection parameter. The horizontal axis ($\epsilon = 0$)corresponds to the perfect Z_2 symmetry. For $\mu < 0$ a symmetric limit cycle labeled 10 collides with the saddle at $\mu = 0$, forming a homoclinic curve with two closed loops, and for $\mu > 0$ splits into two asymmetric limit cycles, labeled 0 and 1. For $\epsilon \neq 0$ splits into two separate single loop homoclinic bifurcations, corresponding to the solid straight lines in Fig. 3. these lines delimit four regions. Two of them are are extensions of the symmetric case, and contain the single limit cycle 10 or the two limit limit cycles 1 and 0which are no longer symmetrically related.In the two additional regions only one cycle limit exists, 1 and 0 respectively. There exist two additional cusp-shaped, where two two limit cycles coexist, 1 and 10, and 0 and 10, respectively. The three limit cycles $(0, 1, 10)$ involved in the gluing bifurcation in the symmetric case give rise to three branches of limit cycles that disappear in homoclinic bifurcations (collision of the limit cycle with a saddle) when $\epsilon \neq 0$, corresponding to the solid lines in Fig. 3, where the dotted line corresponds to a typical path in presence of a fixed imperfection ($\epsilon \neq 0$).

As it can be seen in Fig. 2, over the range of Ri and ϵ where $\mathbb{T}^3$ exist $\mathrm{T_{VLF}} = 2\pi/\omega_{VLF}$ experiences dramatic changes. For $\epsilon = 0$ there are two Ri values where $\mathrm{T_{VLF}}$ becomes unbounded. For $\epsilon \neq 0$, the $\mathrm{T_{VLF}} \to \infty$ splits into three homoclinic bifurcations. The range in Ri where the 1 and 10 $\mathbb{T}^3$ coexist, which corresponds to the width of the cusp region in Fig. 3, is very narrow for the considered imperfections and so the the two distinct homoclinic bifurcations appear to coincide on the scale of the graphics in Fig. 2. For $\epsilon = 10^{-6}$ the width in Ri of the cusp coincidence region is 5.44×10^{-5} and for $\epsilon = 3 \times 10^{-6}$ it becomes 2.4×10^{-5}.

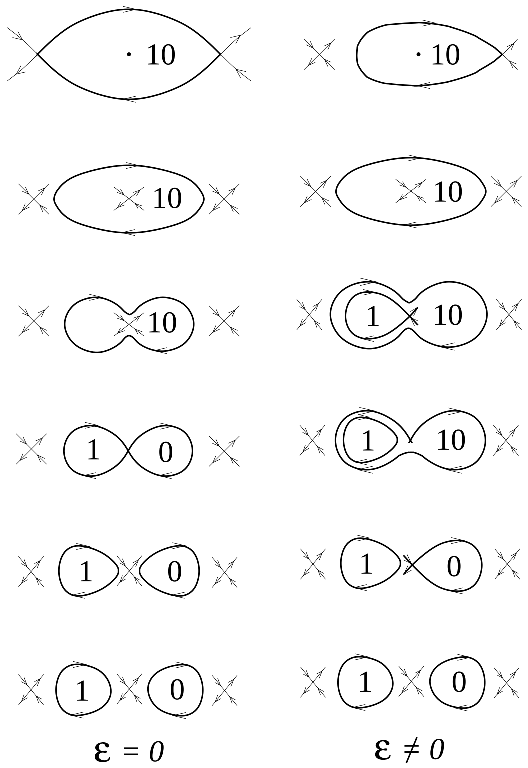

Figure 4: Schematic of the bifurcation sequence for the $\mathbb{T}^3$. $\mathbb{T}^3$ are represented as cycles and $\mathbb{T}^2$ as fixed points.

Figure 4 illustrates schematically the sequences of bifurcations on the $\mathbb{T}^3$ branches. The first column in the figure corresponds to the symmetric case ($\epsilon = 0$), reported in Refs. [2] and [3]. The infinite-period at Ri_{het} bifurcation corresponds to a heteroclinic loop connecting two saddle $\mathbb{T}^2$ related to each other via the temporal glide-reflection symmetry. The $\mathbb{T}^3$ emerging for higher Ri values (10) is invariant, and undergoes a gluing bifurcation Ri_gl. For larger Ri values two asymmetric $\mathbb{T}^3$ exist, 1 and 0. These $\mathbb{T}^3$ solutions become unstable beyond $Ri = 281.26$, and the system evolves towards a $\mathbb{T}^2$ branch.The second column in Fig. 4 represents the imperfect ($\epsilon \neq 0$) case. Both the gluing and the heteroclinic bifurcation become standard homoclinic bifurcations, and there are three different branches $(10, 0, 1)$ that overlap for different values of Ri in agreement with the theoretical description in Fig. 3.

For the particular case here considered, the branch of symmetrical $\mathbb{T}^3$ labeled10 undergoes a closeby (at lower Ri) heteroclinic global bifurcation, and when ϵ increases, the two global bifurcations at either end of this branch collide and the $\mathbb{T}^3$ labeled 10 disappears (at $\epsilon = 5 \times 10{-}6$ and $Ri \simeq 280.93$). This collision of global bifurcations (in this case of two homoclinic bifurcations) alters the bifurcation diagram, dramatically reducing the parameter range of validity of the standard unfolding of the gluing bifurcation.

The conclusion was that in an experiment with even very small levels of imperfection, complex spatio-temporal dynamics can be present that are not obviously associated with the underlying gluing bifurcation. The attempt to establish this relation is presented here.

As the imperfection parameter ϵ increases, some branches disappear and new bifurcations give rise to new branches, whose aspect is less and less symmetric. For ϵ of order 10^{-4} there only remains a robust branch of $\mathbb{T}^3$ (labeled $T3m$ in figure 5), and it undergoes a homoclinic bifurcation only for $\epsilon \leq 1.2 \times 10^{-4}$ to $\mathbb{T}^2$, with $\mathrm{T_{VLF}} \to \infty$. Homo and heteroclinical global bifurcations do not exist anymore for $\epsilon \geq 1.3 \times 10^{-4}$. These global bifurcations become local, usually Neimark-Sacker or saddle-node bifurcations of $\mathbb{T}^2$ and $\mathbb{T}^3$. This is the new feature we are exploring in detail in the present work.

Figure five is a schematic of the existing solutions for two different values of ϵ. For every value of ϵ there

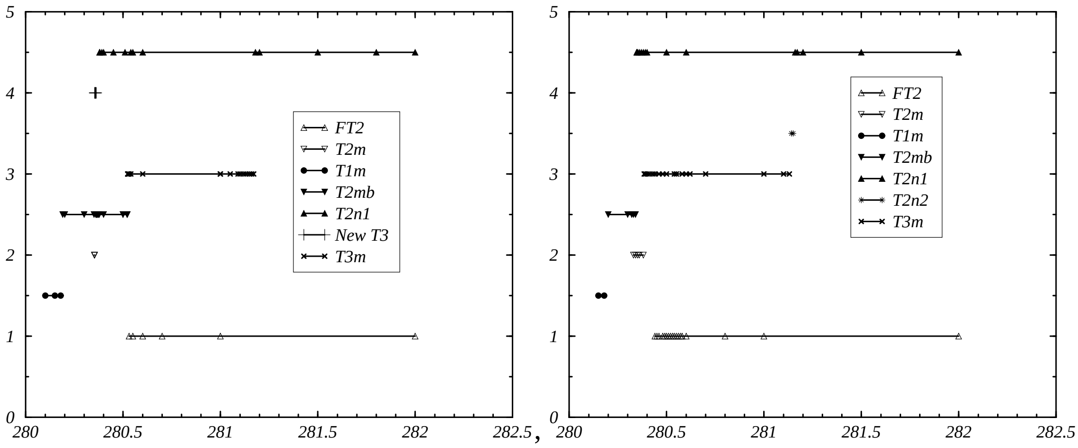

Figure 5: The existing branches for $\epsilon = 1.2 \times 10^{-4}$ and $\epsilon = 1.8 \times 10^{-4}$ respectively.

are common branches like $T2n1$ and $FT2$, that come from the two symmetric $\mathbb{T}^2$ branches for $\epsilon = 0$. These branches are very robust, and increasing enough the Reynolds number, all the $\mathbb{T}^3$ disappear and only these $\mathbb{T}^2$ branches remain, as shown in figure 5.

$T1$ is the basic flow, a periodic limit cycle synchronous with the forcing. This limit cycle undergoes a Neimark-Saker bifurcation to the $T2mb$ branch, that comes from the symmetric $\mathbb{T}^2$ branch for $\epsilon = 0$. For ϵ small, as in figure 5(a), this $T2mb$ branch undergoes a homoclinic bifurcation to the $\mathbb{T}^3$ branch $T3m$. For larger values of ϵ, as in figure 5(b), the bifurcation from $T2mb$ to $T3m$ becomes a Neimark-Saker bifurcation of $\mathbb{T}^2$.

The other branches in figure 5 exhibit a complicated dynamics, including lokings of $\mathbb{T}^2$ and $\mathbb{T}^3$, and the interconnection between the different branches is the subject of our current research.

REFERENCES

[1] F. Marqués, J.M. Lopez, V. Iranzo *Imperfect gluing bifrcation in a temporal glide-reflection symmetric Taylor-Couette flow*, Physics of Fluids Letters, **14**, L33-L36, doi: 10.1063/1.1476915, 2002.

[2] J.M. Lopez, F. Marqués *Dynamics of 3-tori in a periodically forced Navier-Stokes flow*, Phys. Rev. Let. **85**, 972-975, 2001. Theoret. Comput. Fluid Dynamics **16(1)**, 59-69, 2002.

[3] F. Marqués, J.M. Lopez, J. Shen *A periodically forced flow displaying symmetry breaking via a T3 gluing bifurcation and T2 resonances*, Physica D, **156**, 81-97.

[4] J. Abshagen, G. Pfister, T. Mullin *Gluing bifurcation in a dynamical complicated extended flow*, Phys. Rev. Lett. **85**, 224501, 2001.

[5] J. von Stamm, U. Gerdts, T. Buzug, G. Pfister *Symmetry breaken and period doubling on a torus in the VLF regime in Taylor-Couette flow*, Phys. Rev. E **54**, 4938, 1996.

[6] D. V. Turaev *Bifurcations of two-dimensional systems dynamical systems close to a system with two separatrix loops*, Russ. Math. Surveys **40**, 243, 1985.

[7] D. V. Turaev, L.P. Shil'nikov *On bifurcations of a homoclinic 'figure eight' for a saddle with a negative saddle value*, Sov. Math. Dokl **34**, 397, 1987.

[8] P. Glendinning, J. Abshage, T. Mullin *Imperfect homoclinic bifurcations*, Phys. Rev. E **64**, 036208, 2001.